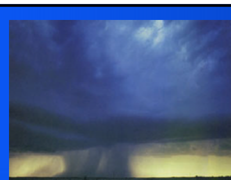

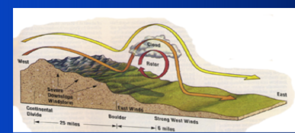

Atmospheric Hazards to Flight

Robert Stengel,
Aircraft Flight Dynamics, MAE 331, 2018

- Microbursts
- Wind Rotors
- Wake Vortices
- Clear Air Turbulence

http://www.princeton.edu/~stengel/MAE331.html
http://www.princeton.edu/~stengel/FlightDynamics.html

Frames of Reference

- **Inertial Frames**
  - **Earth-Relative**
  - **Wind-Relative (Constant Wind)**
- **Non-Inertial Frames**
  - **Body-Relative**
  - **Wind-Relative (Varying Wind)**

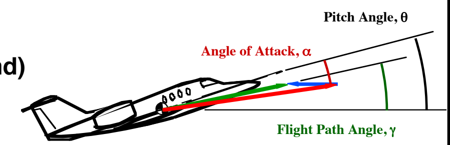

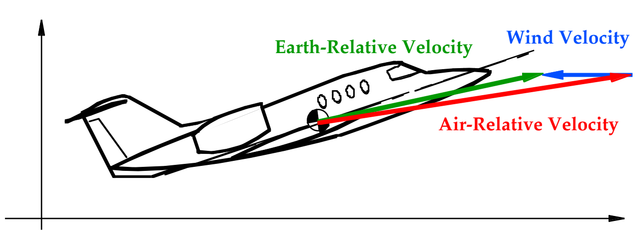

Pitch Angle and Normal Velocity Frequency Response to Axial Wind

- Pitch angle resonance at phugoid natural frequency
- Normal velocity (~ angle of attack) resonance at phugoid and short period natural frequencies

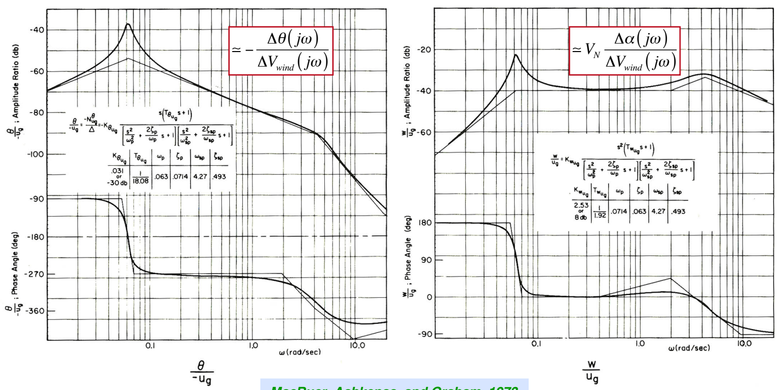

MacRuer, Ashkenas, and Graham, 1973

Pitch Angle and Normal Velocity Frequency Response to Vertical Wind

- Pitch angle resonance at phugoid and short period natural frequencies
- Normal velocity (~ angle of attack) resonance at short period natural frequency

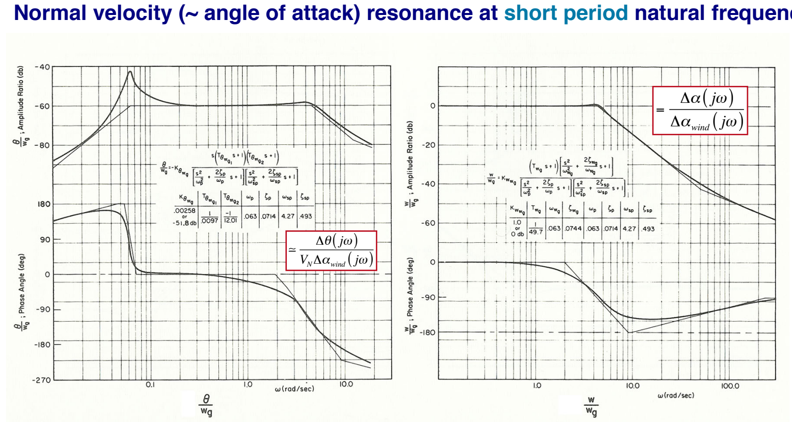

MacRuer, Ashkenas, and Graham, 1973

Sideslip and Roll Angle Frequency Response to Vortical Wind

- Sideslip angle resonance at Dutch roll natural frequency
- Roll angle is integral of vortical wind input

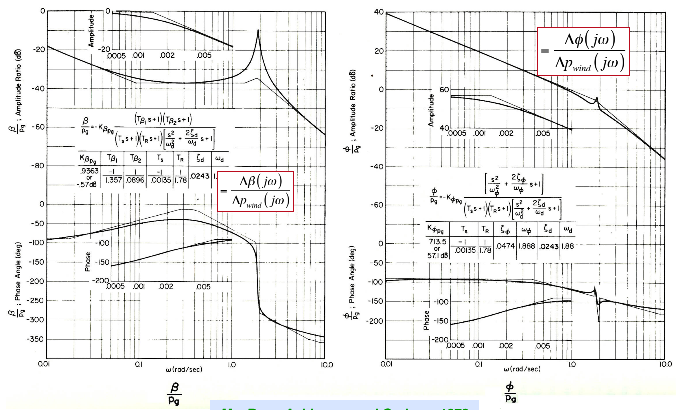

MacRuer, Ashkenas, and Graham, 1973

Sideslip and Roll Angle Frequency Response to Side Wind

- Sideslip and roll angle resonance at Dutch roll natural frequency

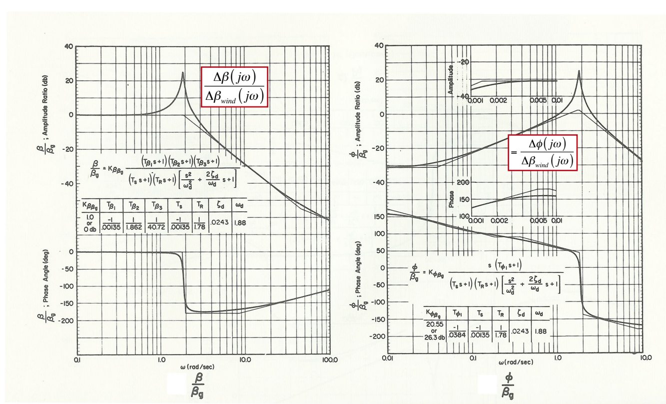

MacRuer, Ashkenas, and Graham, 1973

Microbursts

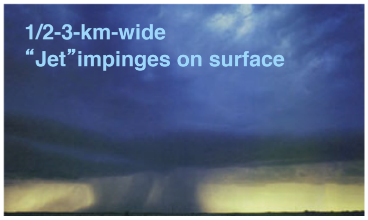

Ring vortex
forms in
outlow

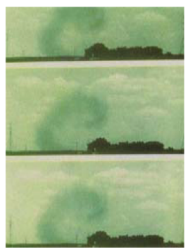

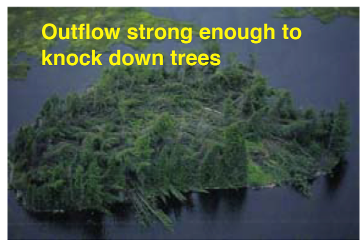

The Insidious Nature of Microburst Encounter

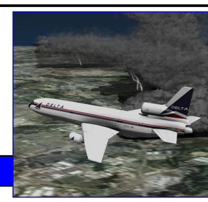

- The wavelength of the phugoid mode and the disturbance input are comparable

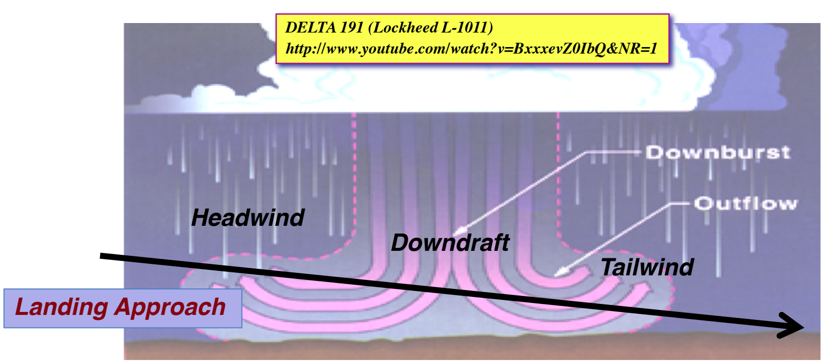

9

Importance of Proper Response to Microburst Encounter

- Stormy evening July 2, 1994
- USAir Flight 1016, *Douglas DC-9*, Charlotte
- Windshear alert issued as 1016 began descent along glideslope

- DC-9 encountered 61-kt windshear, executed missed approach
- Go-around procedure begun correctly -- aircraft's nose rotated up -- but power was not advanced
- Together with increasing tailwind, aircraft stalled
- Crew lowered nose to eliminate stall, but descent rate increased, causing ground impact
- Plane continued to descend, striking trees and telephone poles before impact

http://en.wikipedia.org/wiki/US_Airways_Flight_1016

Importance of Proper Response to Microburst Encounter

- Stormy evening July 2, 1994
- USAir Flight 1016, *Douglas DC-9*, Charlotte
- Windshear alert issued as 1016 began descent along glideslope
- DC-9 encountered 61-kt windshear, executed missed approach
- Plane continued to descend, striking trees and telephone poles before impact
- Go-around procedure was begun correctly -- aircraft's nose rotated up -- but power was not advanced
- That, together with increasing tailwind, caused the aircraft to stall
- Crew lowered nose to eliminate stall, but descent rate increased, causing ground impact

Optimal Flight Path Through Worst *JAWS* Profile

- Graduate research of ***Mark Psiaki***
- Joint Aviation Weather Study (***JAWS***) measurements of microbursts (Colorado High Plains, 1983)
- Negligible deviation from intended path using available controllability
- Aircraft has sufficient performance margins to stay on the flight path

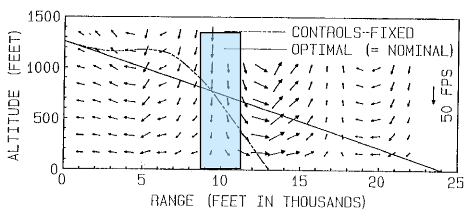

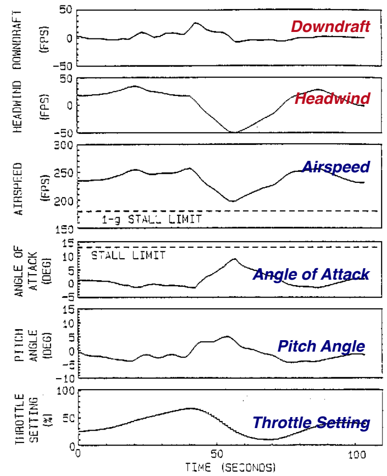

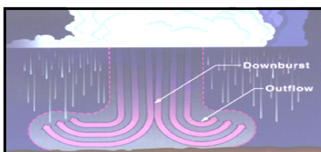

Optimal and 15° Pitch Angle Recovery during Microburst Encounter

- Graduate Research of ***Sandeep Mulgund***
  - Altitude vs. Time

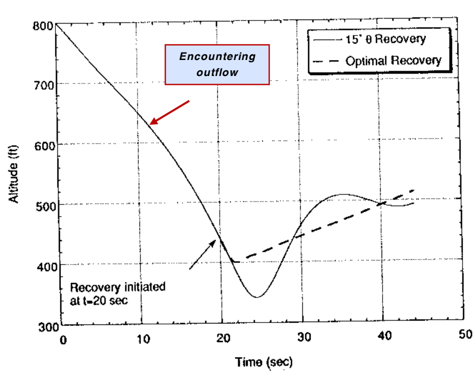

  - Airspeed vs. Time

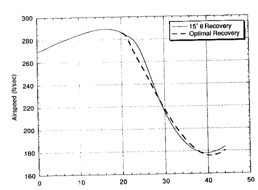

  - Angle of Attack vs. Time

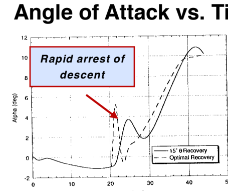

- *FAA Windshear Training Aid*, 1987, addresses proper operating procedures for suspected windshear

Wind Rotors

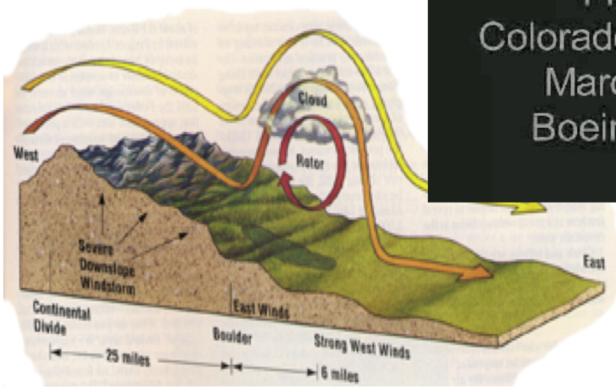

United Airlines
Flight 585
Colorado Springs, CO
March 3, 1991
Boeing 737-200

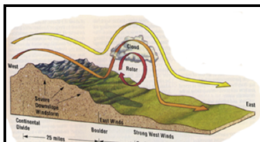

Aircraft Encounters with a Wind Rotor

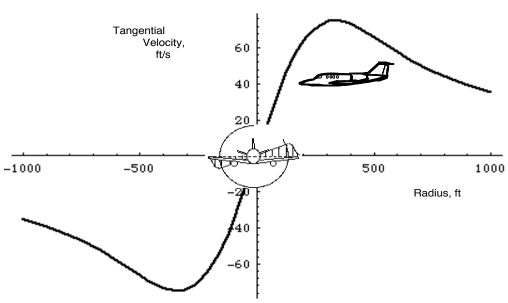

- Tangential velocity vs. radius for *Lamb-Oseen* Vortex

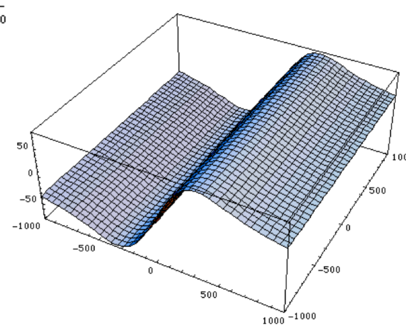

Geometry and Flight Condition of Jet Transport Encounters with Wind Rotor

- Graduate research of *Darin Spilman*
- **Flight Condition**
  - True Airspeed = 160 kt
  - Altitude = 1000 ft AGL
  - Flight Path Angle = -3°
  - Weight = 76,000 lb
  - Flaps = 30°
  - Open-Loop Control
- **Wind Rotor**
  - Maximum Tangential Velocity = 125 ft/s
  - Core Radius = 200 ft

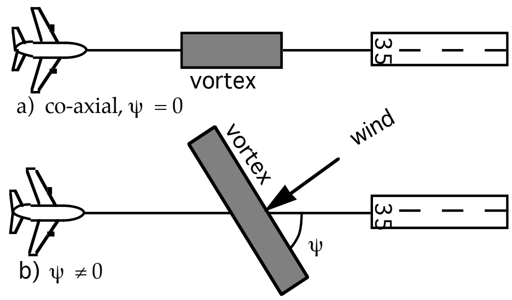

Typical Flight Paths in Wind Rotor Encounter

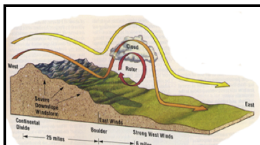

- from *Spilman*

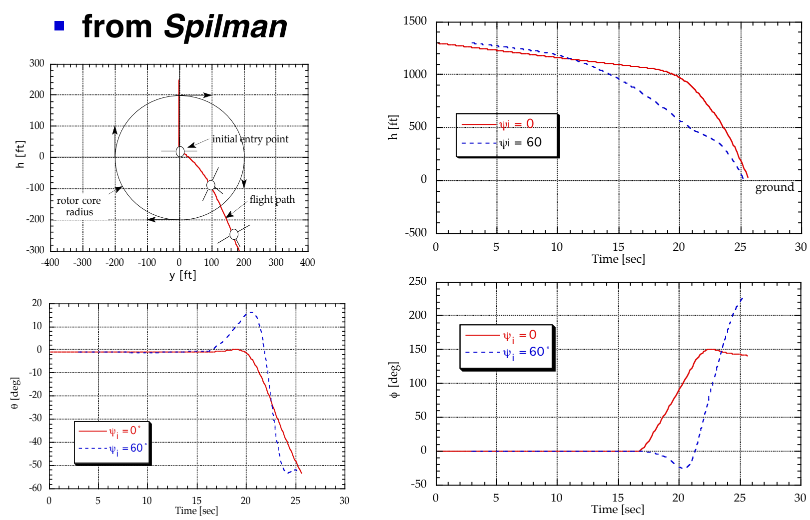

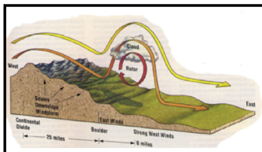

Linear-Quadratic/Proportional-Integral Filter (LQ/PIF) Regulator

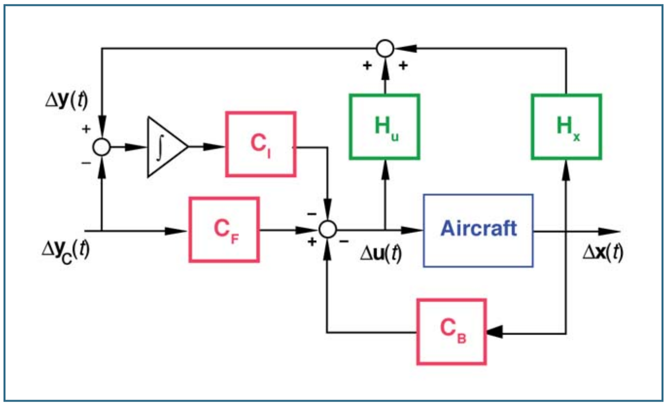

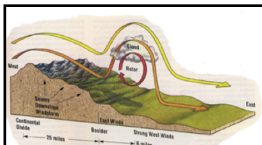

LQ/PIF Regulation of Wind Rotor Encounter

- from *Spilman*

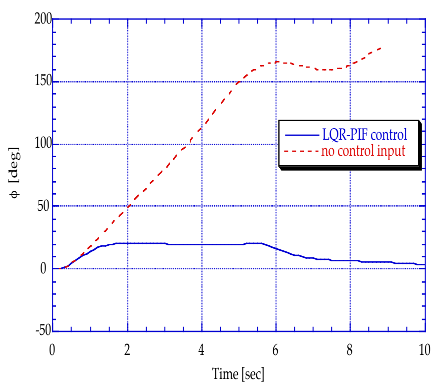

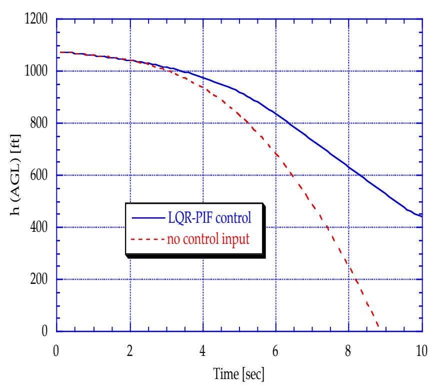

Wake Vortices

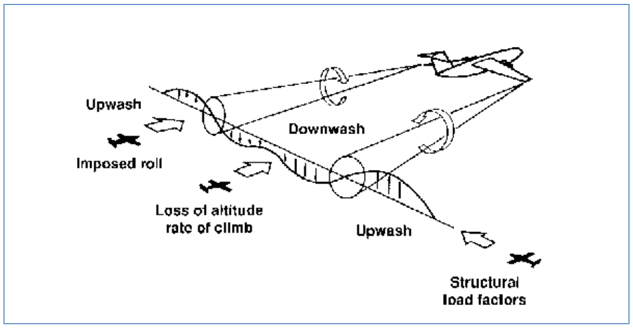

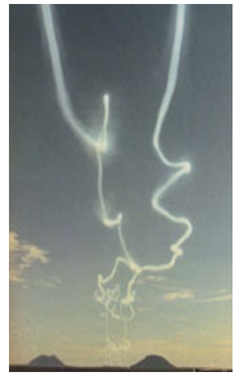

C-5A Wing Tip Vortex Flight Test
https://www.youtube.com/watch?v=uy0hgG2pkUs

L-1011 Wing Tip Vortex Flight Test
https://www.youtube.com/watch?v=AM4R2K7HqOg

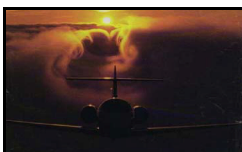

Models of Single and Dual Wake Vortices

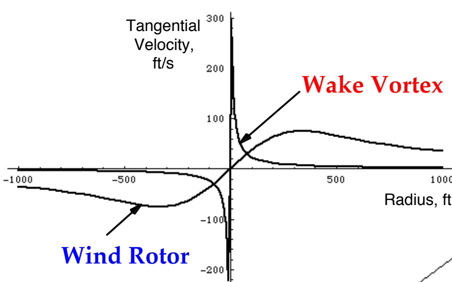

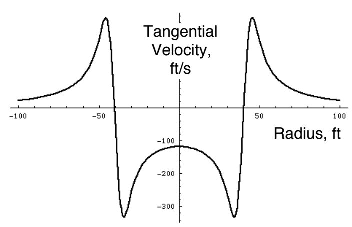

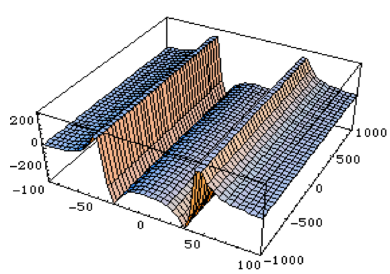

Wake Vortex Descent and Downwash

Wake Vortex Descent and Effect of Crosswind

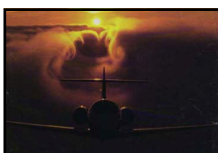

- from *FAA Wake Turbulence Training Aid, 1995*

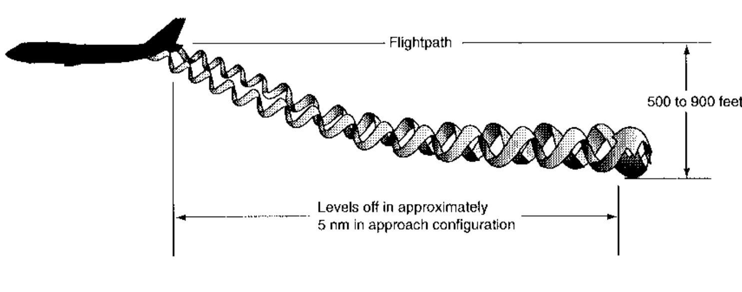

Magnitude and Decay of B-757 Wake Vortex

- **from Richard Page *et al*, FAA Technical Center**

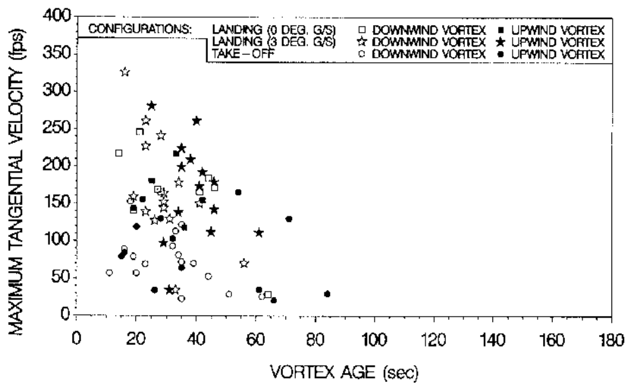

NTSB Simulation of US Air 427 and FAA Wake Vortex Flight Test

- **B-737 behind B-727 in FAA flight test**
- **Control actions subsequent to wake vortex encounter may be problematical**
- **US427 rudder known to be hard-over from DFDR**

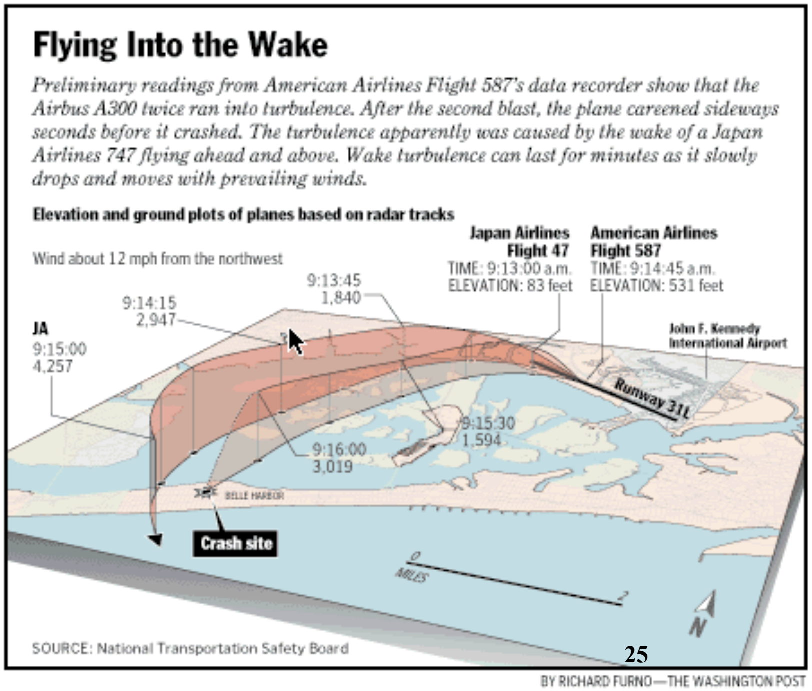

25

NTSB Simulation of American Flight 587

Flight simulation derived from digital flight data recorder (DFDR) tape

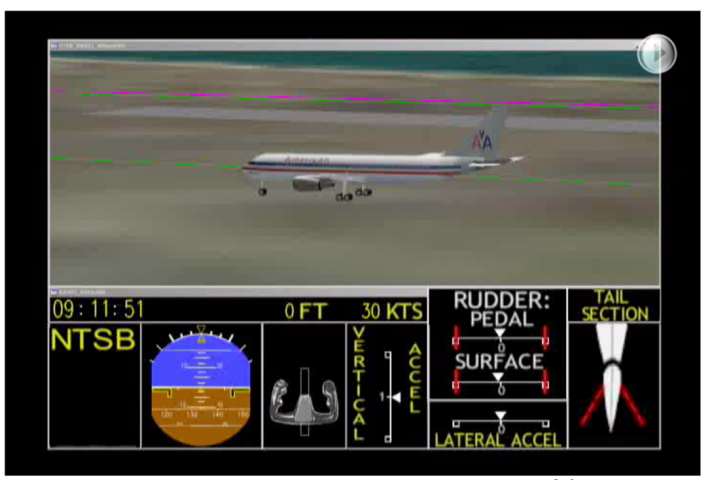

26

Digital Flight Data Recorder Data for American 587

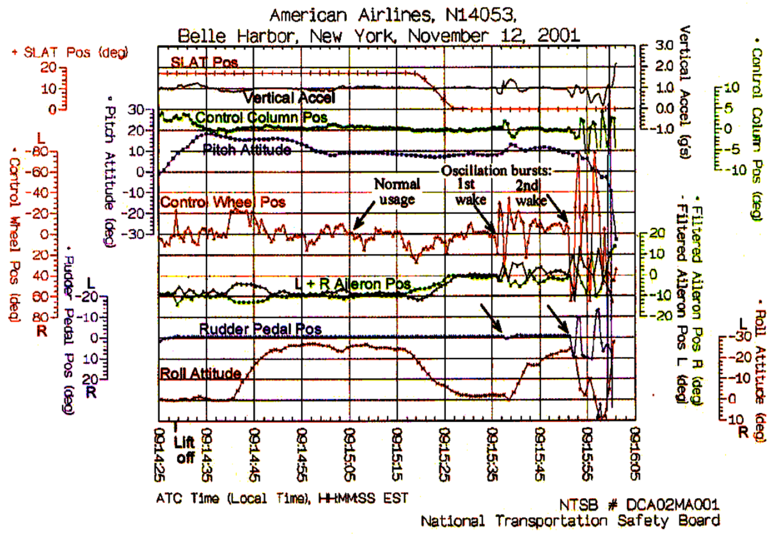

Causes of Clear Air Turbulence

- from *Bedard*

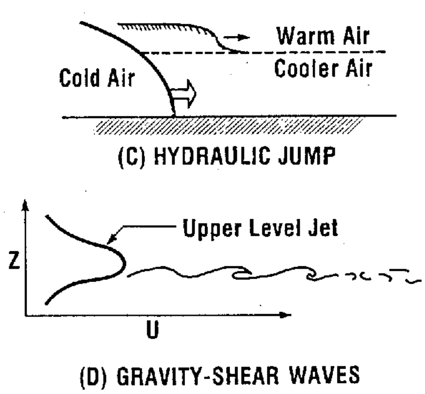

DC-10 Encounter with Vortex-Induced Clear Air Turbulence

- from *Parks, Bach, Wingrove, and Mehta*

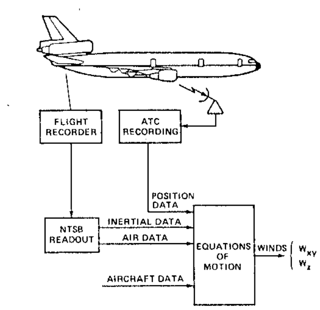

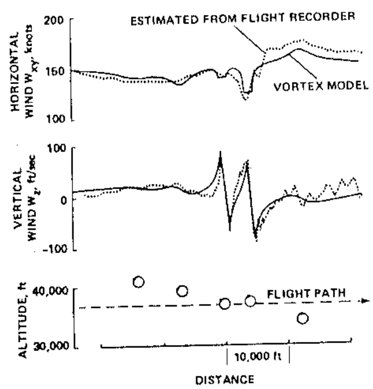

DC-8 and B-52H Encounters with Clear Air Turbulence

- DC-8: One engine and 12 ft of wing missing after CAT encounter over Rockies
- B-52 specially instrumented for air turbulence research after some operational B-52s were lost
- Vertical tail lost after a severe and sustained burst (+5 sec) of clear air turbulence violently buffeted the aircraft
- The Boeing test crew flew aircraft to Blytheville AFB, Arkansas and landed safely

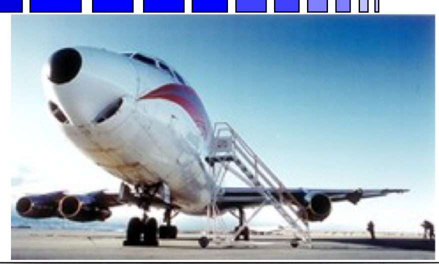

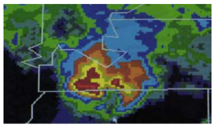

Conclusions

- Critical role of decision-making, alerting, and intelligence
- Reliance on human factors and counter-intuitive strategies
- Need to review certification procedures
- Opportunity to reduce hazard through flight control system design
  - Disturbance rejection
  - Failure Accommodation
- Importance of Eternal vigilance

Supplemental Material

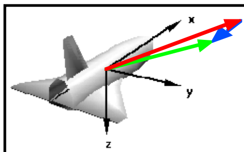

Alternative Reference Frames for Translational Dynamics

- **Earth-relative velocity in earth-fixed polar coordinates:**

$$\mathbf{v}_E = \begin{bmatrix} V_E \\ \gamma \\ \xi \end{bmatrix}$$

- **Earth-relative velocity in aircraft-fixed polar coordinates (zero wind):**

$$\mathbf{v}_E = \begin{bmatrix} V_E \\ \beta_E \\ \alpha_E \end{bmatrix}$$

- **Body-frame air-mass-relative velocity:**

$$\mathbf{v}_A = \begin{bmatrix} (u - u_w) \\ (v - v_w) \\ (w - w_w) \end{bmatrix} = \begin{bmatrix} u_A \\ v_A \\ w_A \end{bmatrix}$$

- **Airspeed, sideslip angle, angle of attack**

$$\begin{bmatrix} V_A \\ \beta_A \\ \alpha_A \end{bmatrix} = \begin{bmatrix} \sqrt{u_A^2 + v_A^2 + w_A^2} \\ \sin^{-1}(v_A / V_A) \\ \tan^{-1}(w_A / V_A) \end{bmatrix}$$

Rigid-Body Equations of Motion

- **Rate of change of Translational Position** $\dot{\mathbf{r}}_I = \mathbf{H}_B^I \mathbf{v}_B$
- **Rate of change of Angular Position** $\dot{\mathbf{\Theta}} = \mathbf{L}_B^I \boldsymbol{\omega}_B$
- **Aerodynamic forces and moments depend on air-relative velocity vector, not the earth-relative velocity vector**
- **Rate of change of Translational Velocity**

$$\dot{\mathbf{v}}_B = \frac{1}{m}\mathbf{F}_B(\mathbf{v}_A) + \mathbf{H}_I^B \mathbf{g}_I - \tilde{\boldsymbol{\omega}}_B \mathbf{v}_B$$

- **Rate of change of Angular Velocity**

$$\dot{\boldsymbol{\omega}}_B = \boldsymbol{I}_B^{-1}\left[\mathbf{M}_B(\mathbf{v}_A) - \tilde{\boldsymbol{\omega}}_B \boldsymbol{I}_B \boldsymbol{\omega}_B\right]$$

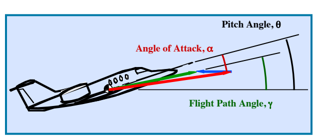

Wind Shear Distributions Exert Moments on Aircraft Through Damping Derivatives

- **3-dimensional wind field** changes in space and time

$$\mathbf{w}_E(\mathbf{x},t) = \begin{bmatrix} w_x(x,y,z,t) \\ w_y(x,y,z,t) \\ w_z(x,y,z,t) \end{bmatrix}_E$$

- **Gradient of wind** produces different relative airspeeds over the surface of an aircraft

$$\mathbf{W}_E = \begin{bmatrix} \partial w_x/\partial x & \partial w_x/\partial y & \partial w_x/\partial z \\ \partial w_y/\partial x & \partial w_y/\partial y & \partial w_y/\partial z \\ \partial w_z/\partial x & \partial w_z/\partial y & \partial w_z/\partial z \end{bmatrix}$$

- **Wind gradient expressed in body axes**

$$\mathbf{W}_B = \mathbf{H}_E^B \mathbf{W}_E \mathbf{H}_B^E$$

$$\Delta C_{l_{shear}} \approx C_{l_{p_{wing}}} \frac{\partial w}{\partial y} - C_{l_{p_{fin}}} \frac{\partial v}{\partial x}$$

$$\Delta C_{m_{shear}} \approx C_{m_{q_{wing,body,stab}}} \frac{\partial w}{\partial x}$$

$$\Delta C_{n_{shear}} \approx C_{n_{r_{fin,body}}} \frac{\partial v}{\partial x}$$

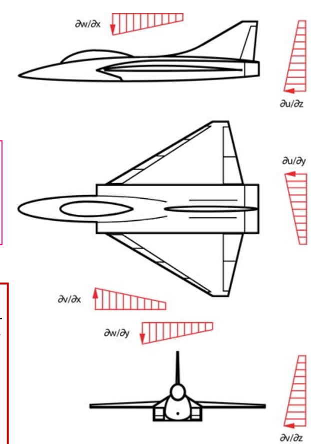

Aircraft Modes of Motion

- **Longitudinal Motions**

$$\Delta_{Lon}(s) = \left(s^2 + 2\zeta\omega_n s + \omega_n^{\,2}\right)_{Ph}\left(s^2 + 2\zeta\omega_n s + \omega_n^{\,2}\right)_{SP}$$

- **Lateral-Directional Motions**

$$\Delta_{LD}(s) = \left(s - \lambda_S\right)\left(s - \lambda_R\right)\left(s^2 + 2\zeta\omega_n s + \omega_n^{\,2}\right)_{DR}$$

- **Wind inputs that resonate with modes of motion are especially hazardous**

Natural frequency: $\omega_n, rad/s$

Natural Period: $T_n = \frac{2\pi}{\omega_n}$, sec

Natural Wavelength: $L_n = V_N\ T_p, m$

Nonlinear-Inverse-Dynamic Control

- **Nonlinear system with additive control:**

$$\dot{\mathbf{x}}(t) = \mathbf{f}\left[\mathbf{x}(t)\right] + \mathbf{G}\left[\mathbf{x}(t)\right]\mathbf{u}(t)$$

- **Output vector:**

$$\mathbf{y}(t) = \mathbf{h}\left[\mathbf{x}(t)\right]$$

- **Differentiate output until control appears in each element of the derivative output:**

$$\mathbf{y}^{(d)}(t) = \mathbf{f}^*\left[\mathbf{x}(t)\right] + \mathbf{G}^*\left[\mathbf{x}(t)\right]\mathbf{u}(t) \triangleq \mathbf{v}(t)$$

- **Inverting control law:**

$$\mathbf{u}(t) = \mathbf{G}^*\left[\mathbf{x}(t)\right]\left[\mathbf{v}_{command} - \mathbf{f}^*\left[\mathbf{x}(t)\right]\right]$$

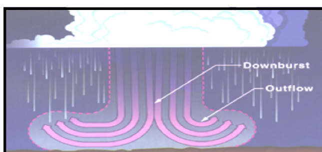

Landing Abort using Nonlinear-Inverse-Dynamic Control

- **from *Mulgund***

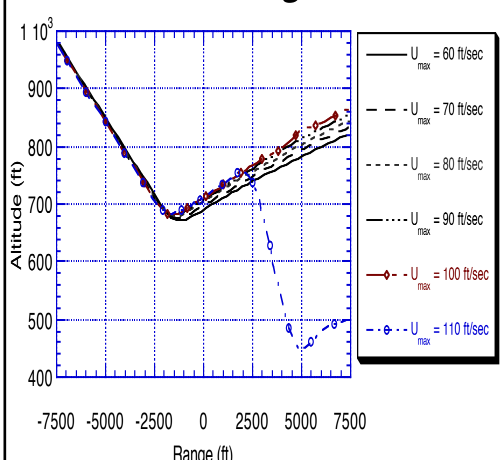

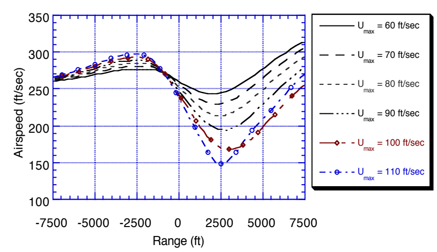

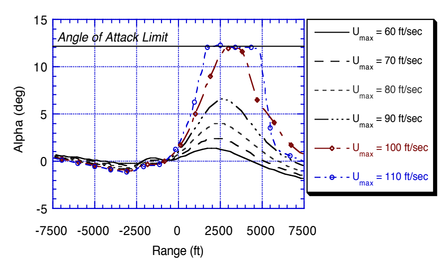

Wind Shear Safety Advisor

- **Graduate research of *Alexander Stratton***
- ***LISP-based expert system***

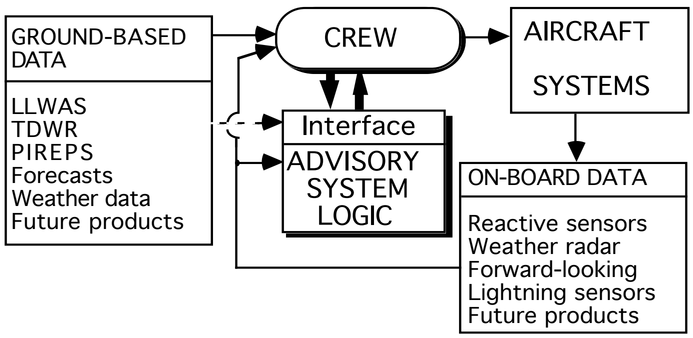

Estimating the Probability of Hazardous Microburst Encounter

- **Bayesian Belief Network**
  - **Infer probability of hazardous encounter from**
    - **pilot/control tower reports**
    - **measurements**
    - **location**
    - **time of day**

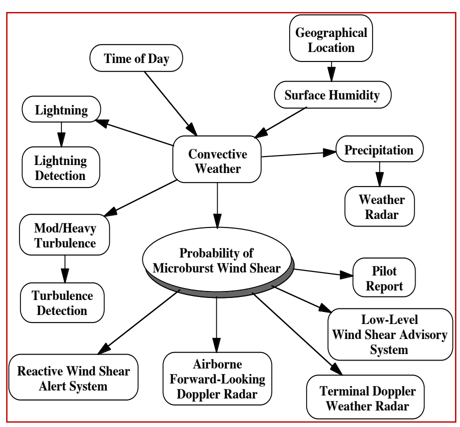

Aircraft as Wake Vortex Generators and Receivers

- **Vorticity, Γ, generated by lift in *1-g* flight**

$$\Gamma = \frac{K_{generator} W}{\rho V_N b}$$

$$K_{generator} \simeq \frac{4}{\pi}$$

- **Rolling acceleration response to vortex aligned with the aircraft's longitudinal axis**

$$\dot{p} = \frac{K_{receiver} \frac{1}{2} \rho V_N^2 S b}{I_{xx}} \Gamma$$

$$K_{receiver} \simeq \frac{C_{L_\alpha}}{2\pi V_N b}$$

Rolling Response vs. Vortex-Generating Strength for 125 Aircraft

- **Undergraduate summer project of *James Nichols***